Optical potentials for alpha particles on heavy nuclei around the Coulomb barrier

M. Avrigeanu (1), W. von Oertzen (2), A.C. Obreja (1), F.L. Roman† (1) and V. Avrigeanu (1)*
(1) "Horia Hulubei" National Institute for Physics and Nuclear Engineering, P.O. Box MG-6, 077125 Bucharest, Romania
(2) Freie Universität Berlin, Fachbereich Physik, Arnimallee 14, 14195 Berlin, and Hahn-Meitner-Institut, Glienicker Strasse 100, 14109 Berlin, Germany

Abstract
A previously semi-microscopic analysis of the α-particle interaction with 50$\leq$ A $\leq$124 target nuclei at energies from $\sim$8 to 50 MeV, based on the Double Folding Model (DFM) for the real part of the optical potential, is extended to heavy nuclei A$\geq$132 nuclei. The energy-dependent phenomenological imaginary part of the corresponding semi-microscopic optical model potential was obtained by taking into account also the dispersive correction to the DFM real potential, and used within a concurrent complete phenomenological analysis of the same data basis. Thus, a phenomenological optical potential was also obtained for the above-mentioned target-nuclei mass and energy ranges, while an ultimate assessment of (α,γ), (α,n) and (α,p) reaction cross sections proves the suitable description of both the low energy elastic-scattering and α-particle induced-reaction data.

1 Introduction

A semi-microscopic analysis of only α-particle elastic scattering on $A\sim$100 nuclei at energies from $\sim$14 to 32 MeV provided also a phenomenological optical model potential (OMP) [1, 2] which describes well the (α,n) reaction data for lighter target nuclei with $A<$54 but led to a major overestimation of similar cross sections [3] for heavier nuclei. Better results were provided in the later cases by either the well-known four-parameter global potential [4] of McFadden-Satchler or also a simpler potential [5], while even the α-particle potential of Galaviz *et al.* [6], which was deduced from the α-particle elastic scattering on ^{112}Sn at energies close to the Coulomb barrier, only poorly describes the α-capture data [3] at energies below 6 MeV. Similar questions are raised by rather recent analyses [7] for target nuclei with A=63-118. A global α-nucleus OMP is proposed by the BARC group [8] for $A\sim$12-209 and energies from Coulomb barrier up to about 140 MeV, based on a previous systematics of the real and imaginary potential volume integrals. The BARC global potential was found to describe well the high energy elastic-scattering data, while at lower energies the calculations and the data differ considerably. An ultimate assessment of (α,γ), (α,n) and (α,p) reaction cross sections, for target nuclei from ^{45}Sc to ^{118}Sn and incident energies below $\sim$12 MeV, has found the actual difficulties as being due to the former diffuseness of the real part of optical potential as well as the surface imaginary-potential depth. Thus, an optical potential which describes equally well both the low energy elastic-scattering and α-particle induced-reaction data was obtained [9] and confirmed [10] by the analysis of additional (α,x) reaction data.

The recent high precision measurements of α-particle elastic-scattering make possible further improvement of global OMPs. We have looked in this respect for an extension of the previous semi-microscopic analysis based on the Double Folding Model (DFM) to the mass region 50$<A<$209 nuclei

*Corresponding author. E-mail: mavrig@nipne.ro Tel.: +40-21-4046125
†Present address: *The DG-KTT Department*, CERN, Geneva, Switzerland

and energies from $\sim$8 to 50 MeV. The energy-dependent phenomenological imaginary part for this semi-microscopic optical potential was obtained including the dispersive correction to the microscopic real potential, and used within a concurrent phenomenological analysis of the same data basis. A global parameter set for low-energy α-particles entirely based on the elastic-scattering data analysis was thus obtained for the nuclei within the above-mentioned mass and energy ranges, and next involved in the reaction data analysis by taking as a starting point the previous OMP parameter values at the lowest energies [9].

2 (α,α) semi-microscopic and phenomenological optical potential analysis

The basic formulas as well as model assumptions for calculations of the DFM real part of the optical potential [11] were discussed already previously [1]. Thus the direct and exchange real parts of the microscopic optical potential are obtained in terms of the projectile and target nuclear densities folded with the M3Y-Reid [12] density- and energy-dependent effective NN-interaction. The knock-on exchange term of the folded potential has been calculated by using the approximation of Campi and Bouyssy [13], which preserves the first term of the expansion given by Negele-Vautherin [14] for the realistic density-matrix, while the average relative momenta of nucleons in the α-particle and in the target are obtained from the modified Thomas-Fermi approximation of Krivine and Treiner [15] for the kinetic-energy density.

Based on the analysis of the α-α elastic-scattering angular distributions measured at incident energies below the reaction threshold, the use of the density distribution of the α-particle of Baye *et al.* [16] provided the better agreement with the data [1]. Finally the nuclear density distribution of the target nuclei has been described by means of a two-parameter Fermi-type function with Negele's [17] parameters chosen to reproduce the electron scattering data.

Similarly to the previous studies [1, 9], within a two-step OMP approach, the semi-microscopic analysis of the α-particle elastic scattering provided the energy-dependent phenomenological imaginary surface and volume potential by using also of the corresponding dispersive correction of Mahaux *et al.* [18] to the DF real potential. It should be emphasized that no adjustable parameter or normalization constant has been involved within this analysis for the OMP real part, in order to preserve the predictive power of the semi-microscopic potential. The consequent comparison between the experimental and semi-microscopical angular distributions for target nuclei from ^{132}Ba to ^{209}Bi is shown in Fig. 1. The computer code SCAT2 [19] has been used in this respect, modified to include the semi-microscopic DF potential. The calculated angular distributions using the OMP parameters of Kumar *et al.* [8] are also shown.

The same imaginary potential has been then involved, in a second step of the OMP approach, within a fully phenomenological analysis of the same data basis. A regional optical potential (ROP) with Woods-Saxon (WS) form factors for the real and imaginary parts has been thus obtained. The advantage of having already well settled the imaginary parameterization of the OMP increases obviously the accuracy of the particular data fit (Fig. 2). Finally, the corresponding averaged well depth and geometry parameters (regional OMP) have been used for calculation of the angular distributions shown in Fig. 2. The deviations of its predictions from the local analysis results may also be seen. These results are compared with those obtained by using the global parameter set of McFadden and Satchler [4], in order to establish the usefulness of the regional OMP. On the other hand, the differences between the predictions of the former ROP [9] devoted to the α-particle interaction with target nuclei $50 \leq A \leq 124$ and those obtained with the present extension for $A \geq 132$ (Fig. 3) are larger for the target masses well beyond the limits of the A-mass range within which it was developed. On the whole, we find that a rather suitable description of the analyzed data is provided by OMPs with real-potential diffuseness a_R [1, 4] notably lower than a_R values which are needed in order to describe α-particle emission from excited compound nuclei [2, 20].

3 (α, x) and total α-reaction cross section analysis

The extended regional potential described above has been involved within the (α,γ),(α,n), and (α,p) reaction cross-sections analysis, at incident energies below the Coulomb barrier. The statistical-model parameters used for the cross section calculations were consistently established by analyzing other various independent experimental data for the nuclei involved. The focus on the uncertainties of α-particle OMP became thus possible. By taking as a starting point the previous OMP parameter values at the lowest energies [9], a suitable description of the excitation functions shown, e.g., in Fig. 4, has been obtained with the only change of the constant value of W_D=(1.5$\pm$0.5) MeV at the lowest energies. An optical potential which describe equally well both the low energy elastic-scattering and induced-reaction data of α-particles on A$\geq$132 target nuclei has finally been obtained for both medium and heavy mass nuclei.

One of the OMP parameter marked by the large sensitivity of statistical-model calculated cross sections is the real-potential diffuseness a_R (e.g., Refs. [2, 9]). The systematics provided by the analysis of the elastic-scattering data for $E_{c.m.}/B_C$ >0.9 imply a real-potential diffuseness increasing with the energy decrease, while the account of measured (α, x) reaction cross sections evidenced a constant a_R value at energies lower than 0.9B_C (slightly changed comparing with those given in Table 3 from Ref. [9]).

The second OMP parameter marked by the largest sensitivity of statistical-model calculated cross sections is the surface imaginary potential depth, W_D [9]. The strong change of the number of open reaction channels close to the Coulomb barrier leads to a strong variation of the imaginary potentials. Therefore, our final change of the extended ROP obtained by elastic-scattering analysis, in order to describe the (α, x) reaction data at energies below Coulomb barrier has been the drop of the surface imaginary potential depth with the decrease of α-particle energy.

4 Conclusions

The previously semi-microscopic analysis of the α-particle interaction with 50$\leq$A$\leq$124 target nuclei, at energies from $\sim$8 to 50 MeV, has been extended to heavy nuclei A$\geq$132 nuclei. The energy-dependent phenomenological imaginary part of the corresponding semi-microscopic optical model potential, obtained by taking into account also the dispersive correction to the DFM real potential, was used within a concurrent complete phenomenological analysis of the same data basis. The phenomenological optical potential which has been thus obtained also for the above-mentioned target-nuclei mass and energy ranges, has been involved within an ultimate assessment of (α,γ), (α,n) and (α,p) reaction cross sections at energies below Coulomb barrier. A suitable description of both the low energy elastic-scattering and α-particle induced-reaction data has been therefore obtained.

Acknowledgments

This work was partly supported by the European Communities within the framework of the European Fusion Development Agreement under Contract of Association between EURATOM-MEdC, and the CNCSIS-Bucharest under Contract No. PN-II-ID-PCE-1-2007-149.

References

[1] M. Avrigeanu, W. von Oertzen, A.J.M. Plompen and V. Avrigeanu, *Nucl. Phys.* **A 723** (2003) 104; M. Avrigeanu and V. Avrigeanu, *Phys. Rev.* **C 73** (2006) 038801.

[2] M. Avrigeanu, W. von Oertzen and V. Avrigeanu, *Nucl. Phys.* **A 764** (2006) 246.

[3] Gy. Gyürky *et al.*, *Phys. Rev.* **C 74** (2006) 025805; N. Özkan *et al.*, *Phys. Rev.* **C 75** (2007) 025801; W. Rapp *et al.*, *Phys. Rev.* **C 78** (2008) 025804.

[4] L. McFadden and G.R. Satchler, *Nucl. Phys.* **A 84** (1966) 177.

[5] T. Rauscher, *Nucl. Phys.* **A 719** (2002) 73c; *Nucl. Phys.* **A 725** (2003) 295(E).

[6] D. Galaviz, Zs. Fülöp, Gy. Gyürky, Z. Máté, P. Mohr, T. Rauscher, E. Somorjai and A. Zilges, *Phys. Rev.* **C 71** (2005) 065802.

[7] M.S. Basunia *et al.*, *Phys. Rev.* **C 71** (2005) 035801; W. Rapp *et al.*, *Phys. Rev.* **C 66** (2002) 015803; S. Harissopulos *et al.*, *J. Phys.* **G 31** (2005) S1417.

[8] A. Kumar, S. Kailas, S. Rathi and K. Mahata, *Nucl. Phys.* **A 776** (2006) 105.

[9] M. Avrigeanu, A.C. Obreja, F.L. Roman, V. Avrigeanu and W. von Oertzen, *At. Data Nucl. Data Tables* **95** (2009) 501; arXiv:0808.0566 [nucl-ex].

[10] M. Avrigeanu and V. Avrigeanu, *Phys. Rev.* **C 79** (2009) 027601; arXiv:0811.0032 [nucl-ex].

[11] Dao T. Khoa and W. von Oertzen, *Phys. Lett.* **B 304** (1993) 8; **B 342**(1995) 6; Dao T. Khoa, W. von Oertzen and H.G. Bohlen, *Phys. Rev.* **C 49** (1994) 1652; Dao T. Khoa, W. von Oertzen and A.A. Ogloblin, *Nucl. Phys.* **A 602** (1996) 98.

[12] G. Bertsch, J. Borysowicz, H. McManus and W.G. Love, *Nucl. Phys.* **A 284** (1977) 399.

[13] X. Campi and A. Bouyssy, *Phys. Lett.* **B 73** (1978) 263.

[14] J.W. Negele and D. Vautherin, *Phys. Rev.* **C 5** (1972) 1472.

[15] H. Krivine and J. Treiner, *Phys. Lett.* **B 88** (1979) 212;

[16] D. Baye, L. Desorgher, D. Guillain and D. Herschkowitz, *Phys. Rev.* **C 54** (1996) 2563;

[17] J.W. Negele, *Phys. Rev.* **C 1** (1970) 1260;

[18] C. Mahaux, H. Ngo and G.R. Satchler, *Nucl. Phys.* **A 449** (1986) 354.

[19] O. Bersillon, Centre d'Etudes de Bruyeres-le-Chatel, Note CEA-N-2227 (1992).

[20] V. Avrigeanu, P.E. Hodgson and M. Avrigeanu, *Phys. Rev.* **C 49** (1994) 2136.

[21] EXFOR Nuclear Reaction Data, http://www-nds.iaea.or.at/exfor.

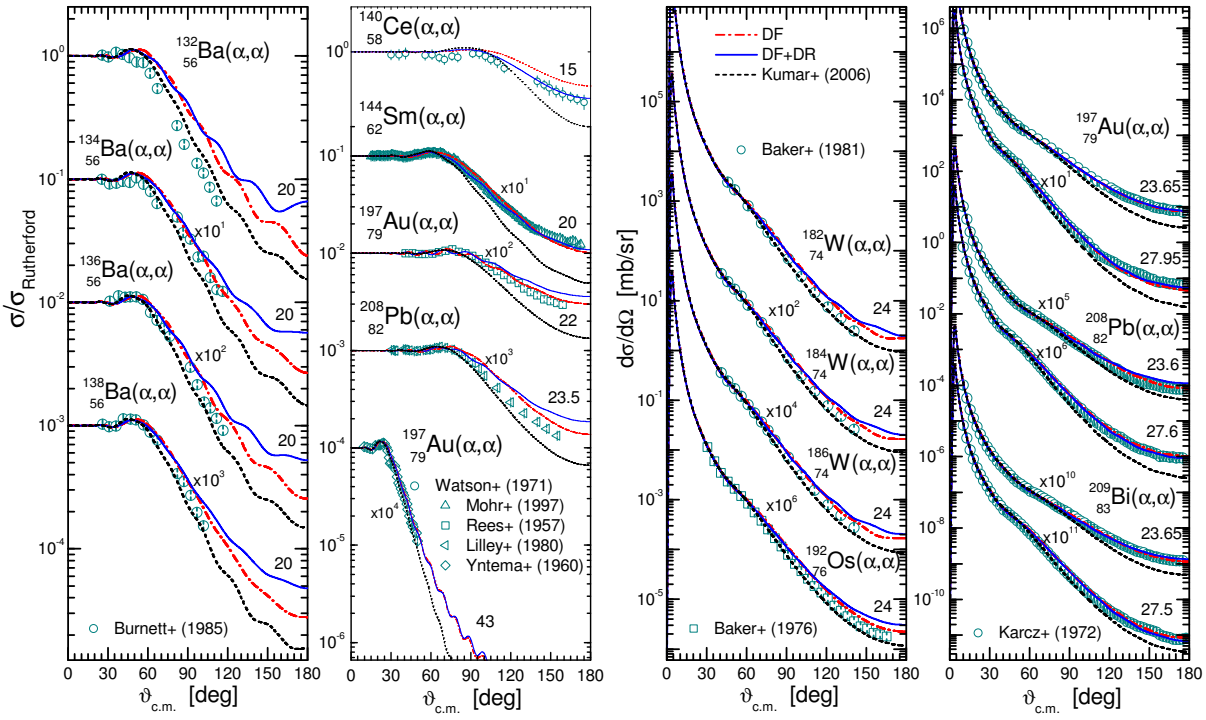

Fig. 1: Comparison of the experimental angular distributions [21] of the elastic scattering of α-particles on ^{132,134,136,138}Ba, ^{182,184,186}W, ^{192}Os, ^{140}Ce, ^{144}Sm, ^{197}Au, ^{208}Pb, and ^{209}Bi between 15 and 43 MeV, with OMP calculations based on either the semi-microscopic approach obtained without (dash-dotted curves) and including the dispersion correction (DR) to the microscopic DF real potential (solid curves), respectively, or by using the OMP parameters of Kumar *et al.* [8] (dotted curves).

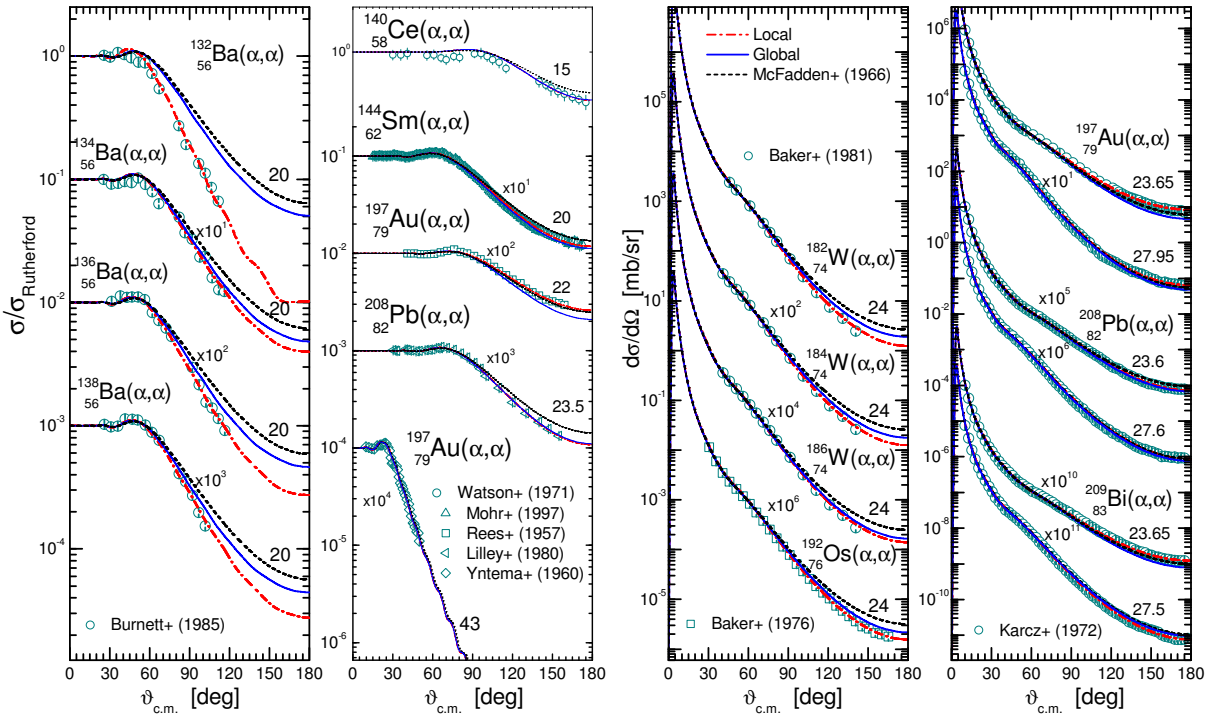

Fig. 2: The same as in Fig. 1, by using the phenomenological local OMP parameters(dash-dotted curves) or the present regional parameter set (solid curves) as well as the global OMP parameter set of McFadden and Satchler [4] (dotted curves).

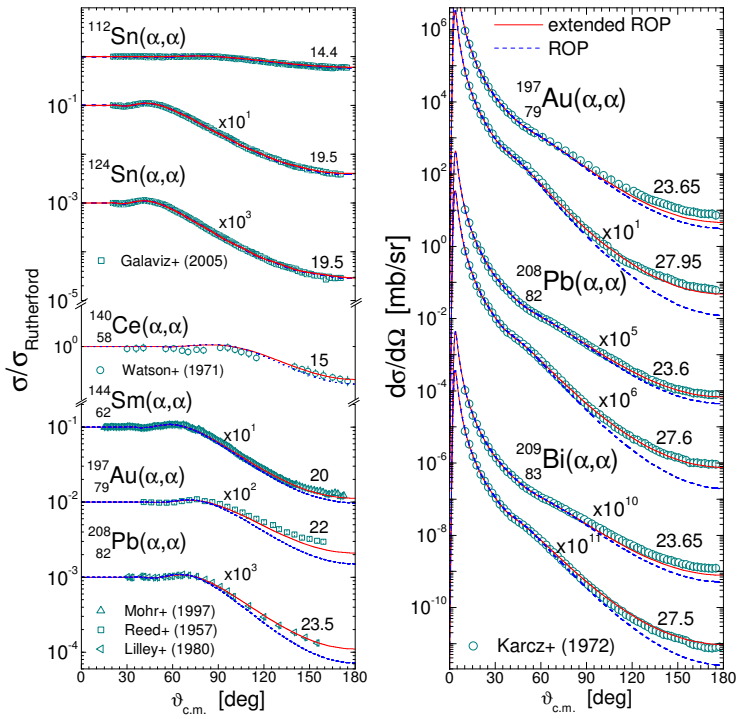

Fig. 3: The differences among the predictions of the former ROP [9] established for the α-particle interaction with $50 \leq A \leq 124$ target nuclei (dashed curves) and those obtained with the present extension for $A \geq 132$ (solid curve).

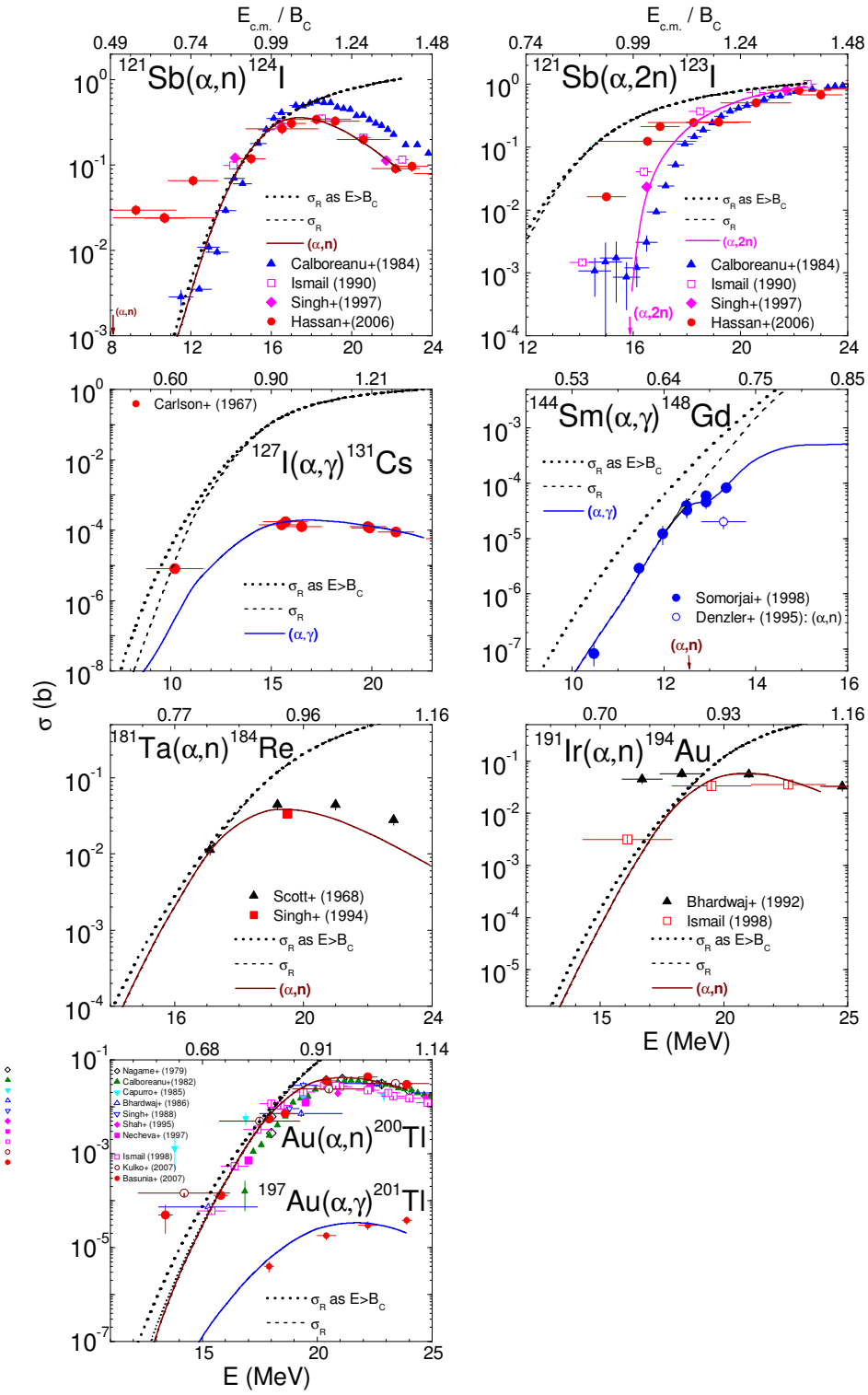

Fig. 4: Comparison of measured (α,γ), (α,n) and $(\alpha,2n)$ reaction cross sections [21] for ^{121}Sb, ^{127}I, ^{144}Sm, ^{181}Ta, ^{191}Ir, and ^{197}Au target nuclei, and calculated values using the predictions of the ROP optical potential established by the elastic-scattering data analysis alone at energies above the Coulomb barrier B_C (dash-dotted curves), and the final ROP proved necessary for the (α,x) reaction data account (solid curves). The total α-reaction cross sections provided at all energies by the ROP parameters established by the elastic-scattering analysis alone, are also shown (dotted curves) for a direct view of the weight of reactions being analyzed, by comparison with the corresponding dash-dotted curves.